J IRAN CHEM SOC (2014) 11:489–498
DOI 10.1007/s13738-013-0322-5

ORIGINAL PAPER

Removal and preconcentration of lead(II), cadmium(II) and chromium(III) ions from wastewater samples using surface functionalized magnetite nanoparticles

Tayyebeh Madrakian · Abbas Afkhami · Nahid Rezvani-jalal · Mazaher Ahmadi

Received: 13 May 2013 / Accepted: 27 July 2013 / Published online: 6 August 2013

Abstract The potential removal and preconcentration of lead(II), cadmium(II), and chromium(III) ions from wastewaters were investigated and explored. Magnetite nanoparticles were chemically modified with *p*-nitro aniline. The aniline-coated magnetite nanoparticles (ANMNPs) were fully characterized by FT-IR, XRD, SEM, and TEM measurements. Batch studies were performed to address various experimental parameters for the removal and determination of these ions. ANMNPs showed high tendency to investigated metal ions, in this order: Cr(III) > Cd(II) > Pb(II), owing to the strong contribution of surface loaded aniline. The potential applications of ANMNPs adsorbent for removal and preconcentration of Pb(II), Cr(III), and Cd(II) from wastewaters as well as drinking tap water samples were successfully accomplished giving recovery values of (98–101 %), without any noticeable interference of the wastewater or drinking tap water matrices.

Keywords Magnetic nanoparticles · Removal · Preconcentration · Heavy metals · Wastewater · *p*-Nitro aniline

Introduction

Heavy metals are released into the environment from industrial applications, including mining, refining, and production of textiles, paints and dyes. High concentrations may have severe toxicological effects on living organisms [1]. Considerable amounts of heavy metals enter the environment from metallurgy industries, combustion of coal, and automobiles. Heavy metals can easily enter the food chain through a number of pathways, and long-term exposure in a contaminated environment can cause progressive toxic effects due to gradual accumulation in living organisms over their life span [2]. Consequently, the development of reliable methods for the removal and determination of heavy metals in environmental and biological samples is of particular significance. The accurate determination of heavy metals at trace levels in environmental samples is one of the aims of analytical chemists, due to their important roles in our life [3, 4].

Flame atomic absorption spectrometry (FAAS) is among the most widely used method for the determination of the heavy metals at trace levels, but the sensitivity and selectivity of FAAS are usually insufficient for the determination of heavy metals at trace concentration in complex matrix environmental samples. In the trace analysis, therefore, preconcentration or separation of trace elements from the matrix is frequently necessary to improve their detection and selectivity by FAAS [5]. The main advantages of preconcentration procedures are increased detection sensitivity at lower analyte concentration and avoidance of the matrix effect due to effective separation of the analyte from interfering matrix components [6].

A number of separation/preconcentration procedures have been used for trace metal determinations; these include precipitation/co-precipitation [7], liquid–liquid extraction [8], and solid phase extraction (SPE) [9–11]. Among these techniques, SPE procedures, either off- or on-line, are considered superior to other procedures for their simplicity, consumption of small volumes of organic solvent, and ability to achieve a higher enrichment factor. The quest for new adsorbents is an important factor in

T. Madrakian (✉) · A. Afkhami · N. Rezvani-jalal · M. Ahmadi
Faculty of Chemistry, Bu-Ali Sina University, Hamedan, Iran
e-mail: madrakian@gmail.com; madrakian@basu.ac.ir

improving analytical sensitivity and precision in SPE techniques. The main requirements for a substance to work effectively as an SPE adsorption material are as follows: it should consist of a stable and insoluble porous matrix having suitable active groups, typically organic groups, which can interact with analytes; it should achieve fast and quantitative sorption; and it should have high adsorption capacity, good regenerability, and surface area accessibility. To date, many adsorbents, such as active carbon [12], modified resin [13], nanometer-sized materials [14], and fullerene [15], have been employed in SPE. These adsorbents are normally modified by attaching organic and inorganic molecules to their surface. The resulting functional materials can work effectively to remove specific toxic metal ions from aqueous media.

Recently, nanometer-sized materials have attracted substantial interest in the scientific community because of their special properties [16]. The size range of nanoparticles is from 1 to almost 100 nm, which falls between the classical fields of chemistry and solid state physics. The relatively large surface area and highly active surface sites of nanoparticles enable them to have a wide range of potential applications, including shape-selective catalysis [17], chromatographic separations [18], and sorption of metal ions [19], enzyme encapsulation [20], DNA transfection [21], and drug delivery [22]. Magnetic nanoparticles, a new kind of nanometer-sized material, are widely used in the fields of biotechnology and biomedicine for applications such as cell labeling and separation [23], magnetic resonance imaging (MRI) (as a contrast agent) [24], enzyme and protein separations [25], targeted drug delivery [26], and magnetic Ferro fluids hyperthermia [27]. These particles are super paramagnetic, which means that they are attracted to a magnetic field, but retain no residual magnetism after the field is removed. Therefore, suspended super paramagnetic particles adhered to the target can be removed very quickly from a matrix using a magnetic field, but they do not agglomerate after removal of the field. Hu et al. [28] employed magnetic Fe_2O_3 nanoparticles as adsorption material for the removal and recovery of Cr(VI) from wastewater, and the adsorption capacity was found to be very high. However, it should be pointed out that pure inorganic nanoparticles (such as Fe_3O_4 and Fe_2O_3) can easily form large aggregates, which may alter their magnetic properties [25]. Moreover, these nanometer-sized metal oxides are not target selective and are unsuitable for samples with complicated matrices [29]. Therefore, a suitable coating is essential to overcome such limitations.

In this study, aniline-coated magnetite nanoparticles (ANMNPs) were synthesized according to our previous literature [32]. These magnetic nanoparticles were employed as an SPE adsorbent for separating and concentrating trace amounts of Pb(II), Cd(II), and Cr(III) ions from environmental samples. The levels of these elements were then determined by FAAS. Experimental data obtained from batch equilibrium tests have been analyzed by different sorption isotherm models, namely Langmuir, Freundlich, Sips, and Redlich–Peterson isotherms. The effects of various parameters such as pH of the solutions, amount of adsorbent and contact time on the adsorption process were studied and interpreted.

Experimental setup

Reagents and apparatus

All the chemicals used were of analytical reagent grade or the highest purity available and were purchased from Merck Company (Darmstadt, Germany). Aqueous solutions of chemicals were prepared with deionized water. All glassware were soaked in dilute nitric acid for 12 h and then thoroughly rinsed with DDW. Standard solutions of Pb(II), Cd(II), and Cr(III) ions were prepared from the nitrates of these elements each as 1,000 mg L^{-1}. Working solutions, as per the experimental requirements, were freshly prepared from the stock solution for each experimental run. The adjustments of pH were performed with 0.01–1.0 mol L^{-1} HCl and NaOH solutions.

The concentration of metals was determined by atomic absorption spectrometry using an Aurora model Spect AI 1200 apparatus. The instrumental settings of the manufacturer were followed. Infrared spectra were recorded with a Fourier transform infrared spectrometer (FT-IR, Perkin Elmer, Spectrum 100, UK). Samples were gently ground and diluted in nonabsorbent KBr matrices to identify the functional groups and chemical bonding of the coated materials. The size, morphology and structure of the nanoparticles were characterized by transmission electron microscopy (TEM, Philips, CM10, the Netherlands, 100 kV) and scanning electron microscopy (SEM, Philips, XL30, the Netherlands). The crystal structure of the synthesized materials was determined by an X-ray diffractometer (XRD) [38066 Riva, d/G.Via M. Misone, 11/D (TN) Italy] at ambient temperature. A Metrohm model 713 (Herisau, Switzerland) pH meter with a combined glass electrode was used for pH measurements.

Preparation of samples

Preparation of natural and sewage water samples

The KWC wastewater (collected from KWC Co., Arak, Iran), radiator manufacturing wastewater (collected from Arak, Iran), and tap water (collected from our faculty) were immediately filtered through Millipore cellulose membrane

filter (0.45 μm pore size), acidified to pH 2.0 with HNO_3, and stored in precleaned polyethylene bottles. After then, pH of the sample was adjusted to 5.0 and analyzed by the recommended procedure.

For rice samples (Iranian Hashemi's rice), 1.0 g of the sample was weighed and powdered. Then 15 mL of concentrated HNO_3 was added and the mixture was kept overnight. Then, 6 mL of concentrated HNO_3 and 4 mL of concentrated $HClO_4$ were added to the beaker. It was evaporated near to dryness on a hot plate at about 130 °C for 3 h. The residue was dissolved in 0.5 mol L^{-1} HNO_3 and filtered. The clear solution obtained was diluted to 50 mL with distilled water [30].

Preparation of nanostructured magnetite

The magnetite nanoparticles (MNPs) were prepared by the conventional co-precipitation method with minor modifications [31].

Preparation of aniline-coated magnetite nanoparticles (ANMNPs)

Functionalization of magnetite nanoparticles by *p*-nitro aniline was performed according to our previous literature [32] with some modifications. Primary azo salt of *p*-nitro aniline was prepared by the reaction of nitrous acid (HNO_2) and *p*-nitro aniline at +4 °C. Then this salt reacts directly with magnetite in basic solution according to Scheme 1. A suitable amount of *p*-nitro aniline (0.5 mmol, 0.313 g) and 1 mL of 1 mol L^{-1} HCl in 5 mL DDW was treated and stirred in the ice bath. Then 3 mmol of $NaNO_2$ (0.210 g) in DDW (5 mL) was added and the mixture was stirred at +4 °C for 10 min. The resulting diazonium salt solution was poured into a +4 °C mixture of 0.5 g magnetite in 3.75 mmol of NaOH (5 mL) solution. The mixture was stirred in the ice bath for 30 min. The precipitate (nitrobenzene-coated magnetite nanoparticles, NBMNPs) was filtered off, washed with NaCl, DDW, and ethanol and dried in vacuum. Then a mixture of NBMNPs (3.52 g), NH_4Cl (1.07 g), and 10 mL of H_2O in 100 mL of ethanol was heated to boiling point and zinc dust (2.0 g) in 0.1 g portions at intervals of several minutes was added. The mixture was then refluxed for 5 h. The resulting ANMNPs were magnetically filtered, washed with DDW and dried in vacuum [33].

Recommended procedure for sorption and desorption of heavy metal ions

A series of 300 mL sample solutions containing heavy metal ions were transferred into a 500 mL beaker. The pH of the solution was adjusted to 5.0 using 0.01–0.1 mol L^{-1} HCl and/or NaOH solutions. After that, optimum weight of the adsorbent (0.03 g for Pb^{2+} and 0.07 g for Cd^{2+}, and Cr^{3+} ions) was added to the solution and the mixtures were dispersed by ultrasonication for 90 min at room temperature to attain equilibrium and then magnetically separated. Then, the sorbent was washed with deionized water and afterward, the metal ions retained on adsorbent were eluted with the solution of the mixture of 4.0 mL from mixture of methanol:0.1 mol L^{-1} HNO_3 (1:1 v/v). The analytes in the eluate were then determined by FAAS.

Results and discussion

Characterization of the adsorbent

The FT-IR spectra of magnetite nanoparticles, NBMNPs, and ANMNPs are presented in Fig. 1. As can be seen, after grafting of *p*-nitro aniline on the Fe_3O_4 (Fig. 1a), a new peak was appeared at 1,597 cm^{-1} that indicated the C=C stretching of aromatic ring of *p*-nitro aniline on the Fe_3O_4 (Fig. 1b). At 1,346 and 1,519 wavenumbers the N–O groups and at 3,080 and 3,108 cm^{-1} C–H aromatic stretching of *p*-nitro aniline were present, emphasizing that the NBMNPs was synthesized.

After reduction of nitro groups to primary amine group, as can see from Fig. 1c, the peaks at 1,346 and 1,519 wavenumbers disappeared, indicating that nitro group is reduced to primary amine group. But because broad peak of hydroxyl groups of nanoparticles overlaps with primary amine group peaks, this peak cannot be observed. In order to prove the existence of $–NH_2$ groups, ANMNPs was reacted with benzaldehyde to form the corresponding Schiff base [34]. Figure 1d shows the FT-IR of the Schiff base. As can be seen a new peak at about 1,636 cm^{-1} (–N=C– group) appears proving the formation of Schiff base and proving that primary amine groups was formed at ANMNPs.

The SEM and TEM images of the ANMNPs are presented in Fig. 2. TEM image revealed that the diameter of the synthesized nanoparticles were around 20–25 nm (Fig. 2b).

The crystallite size was obtained as 17 nm from the XRD pattern according to Scherrer equation and all the diffraction peaks are consistent with the seven diffraction peaks at (2 2 0), (3 1 1), (4 0 0), (4 2 2), (5 1 1), (4 4 0), and (5 5 3) by comparison with joint committee on powder diffraction standards (JCPDS card, file No. 79-0418), which are indexed to the cubic spinel phase of Fe_3O_4 (Fig. 3).

Effect of solution pH

One of the important factors affecting on the removal of cations from aqueous solutions is the pH of the solution.

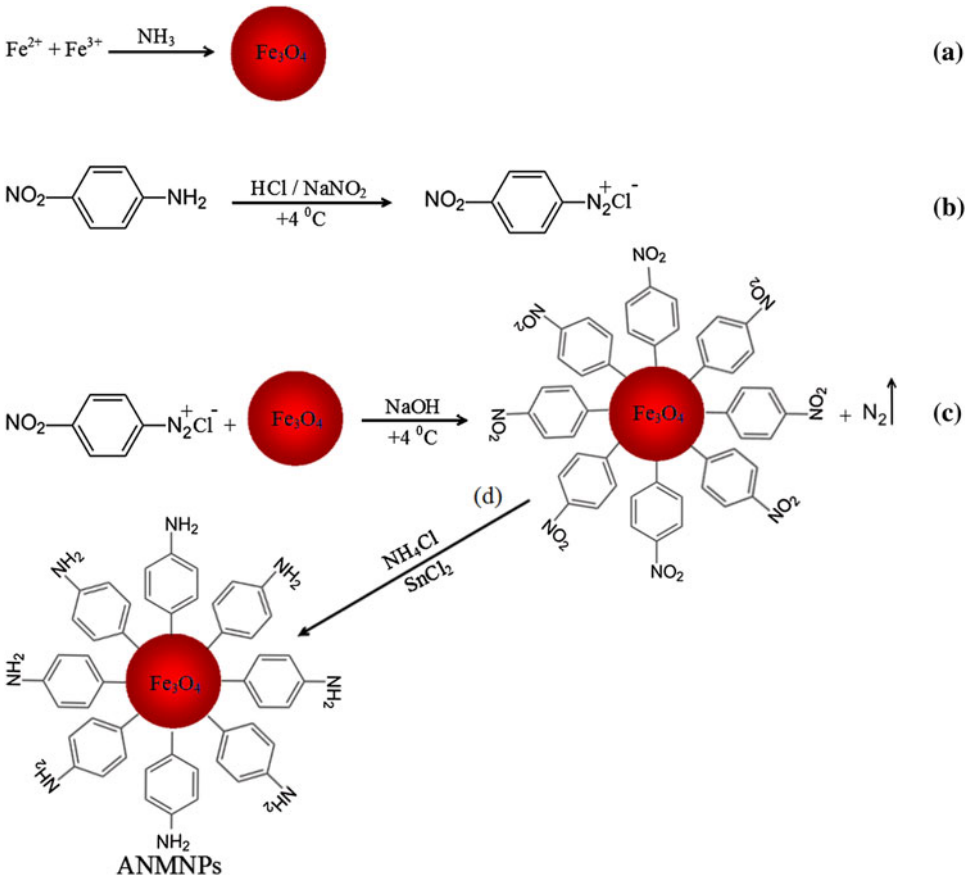

Scheme 1 Synthesis of **a** magnetite nanoparticles, **b** diazonium salt, **c** nitrobenzene-coated magnetite nanoparticles (NBMNPs), and **d** reduction of NBMNPs to ANMNPs

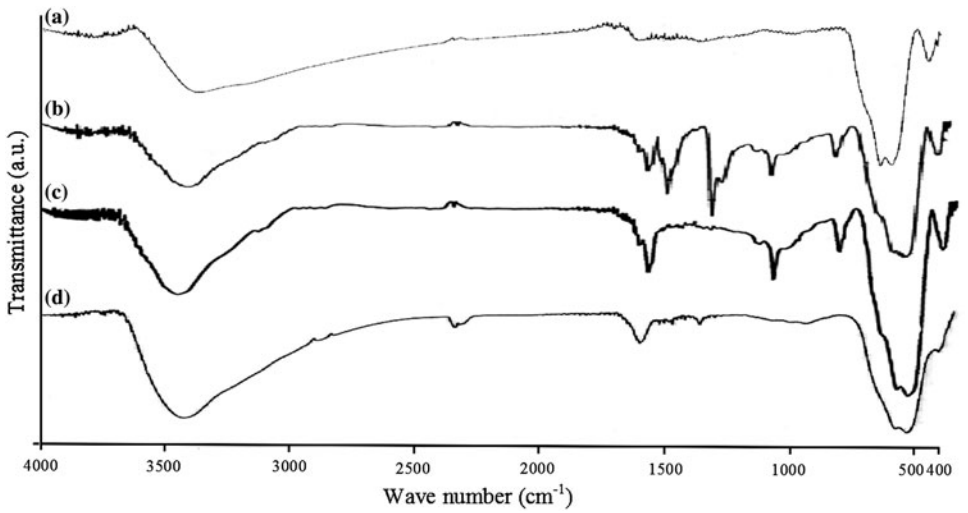

Fig. 1 FT-IR spectra of *a* magnetite nanoparticles, *b* NBMNPs, *c* ANMNPs, and *d* product of Schiff base test

The dependence of metal sorption on pH is related to both the metal chemistry in the solution and the ionization state of the functional groups of the sorbent which affects the availability of binding sites [35].

In order to evaluate the influence of this parameter on the adsorption of cations, the experiments were carried out with the pH range of 3.0–5.5. A 0.05-g sample of adsorbent was suspended in 50 mL solution of 25 mg L^{-1} each of metal ions at several pH values (3.0, 3.5, 4.0, 4.5, 5.0, and 5.5) using either 0.1 mol L^{-1} NaOH or 0.1 mol L^{-1} HCl for pH adjustment. These samples were stirred for 60 min. Then the samples were magnetically filtered out.

The effect of pH on adsorption efficiencies is shown in Fig. 4. The pH range was chosen as 3.0–5.5 to avoid precipitation of metal cations in the form of chloride or hydroxide metals. Removal of Pb(II), Cd(II), and Cr(III)

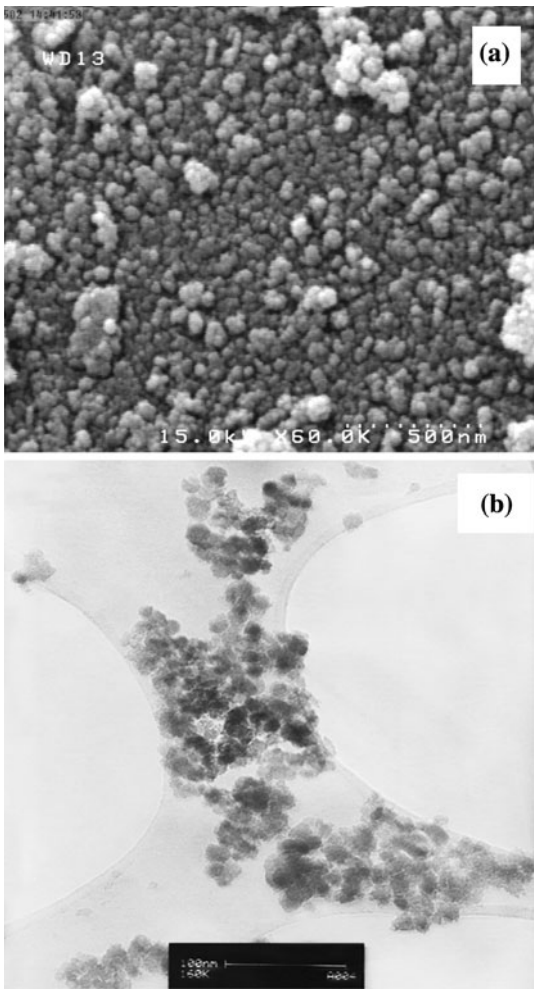

Fig. 2 SEM image (**a**) and TEM image (**b**) of ANMNPs nanoparticles

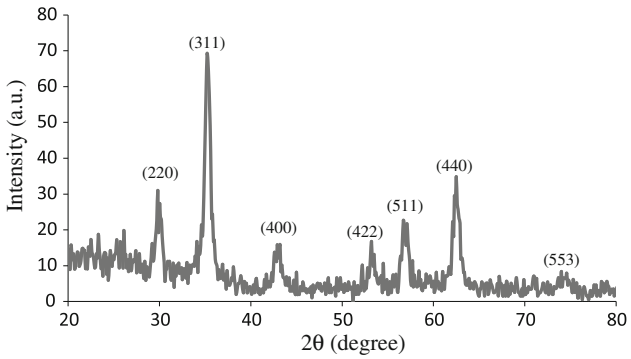

Fig. 3 The XRD pattern of ANMNPs

increases with increasing solution pH and a maximum value was reached at an equilibrium pH of around 5.0. A weak adsorption occurs in acidic medium but it can be seen that higher pH leads to higher metal uptake. Acidic conditions are not favorable because most of the functional groups of the components ($-NH_2$) are protonated leaving

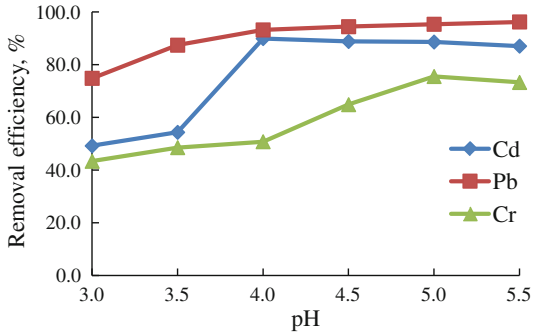

Fig. 4 Removal efficiency at different pHs. Conditions: 0.05 g adsorbent, 50 mL of 25.0 mg L^{-1} of heavy metal ions, agitation time of 60 min

few available ionized groups [35]. Competition between protons and metal species could thus explain the weak adsorption in acidic medium. The highest uptake value was recorded at the pH 4.0 and 5.0. This may be attributed to the presence of free lone pair of electrons on nitrogen and deprotonated oxygen atoms, which are suitable for coordination with the metal ions. Generally, the metal ions in the aqueous solution may undergo solvation and hydrolysis. The process involved for metal adsorption is as follows [35]:

$$M^{2+} + nH_2O \leftrightarrow M(H_2O)_n^{2+} \quad (1)$$

$$M(H_2O)_n^{2+} \leftrightarrow \left[M(H_2O)_{n-1}(OH)\right]^{+} + H^{+} \quad (2)$$

or totally

$$M^{2+} + nH_2O \leftrightarrow \left[M(H_2O)_{n-1}(OH)\right]^{+} + H^{+} \quad (3)$$

for example, the pK_a value for Pb(II) and Cd(II) are 7.7 and 10.1, respectively. Perusal of the literature on metal speciation shows that the dominant species is $M(OH)_2$ at pH > 6.0 and M^{2+} and $M(OH)^{+}$ at pH < 6.0. Maximum removal of metal was observed at pH 5.0 for adsorption. On further increase of pH, adsorption decreases probably due to the formation of hydroxide of cadmium and lead because of chemical precipitation [35]. To achieve high efficiency and good selectivity, a pH of 5.0 was selected for further works.

Effect of the amount of adsorbent

We studied the dependence of the adsorption of cations on the amount of modified nanoparticles at room temperature and at pH 5.0 by varying the adsorbent amount from 0.01 to 0.09 g in contact with 50 mL solution of the mixture of 25 mg L^{-1} each of cations. The suspension was then stirred for 60 min. After magnetically filtering, the supernatant was analyzed for the remaining cations. The results showed that the percentage removal of cations increased by

increasing the amount of adsorbent due to the greater availability of the adsorbent. The adsorption reached a maximum with 0.03 g of adsorbent for Pb(II) and 0.07 g for Cd(II), Cr(III). And the maximum percentage removal was about 98 %.

Effect of contact time

The importance of stirring time comes from the need for identifying the possible rapidness of binding and removal processes of the tested metal ions by the adsorbents and obtaining the optimum time for complete removal of the target metal ions. The analysis of batch adsorption of metal ions was carried out in 30-min steps and the concentration of each sample was measured by atomic absorption spectroscopy after 120-min contact time. The results were recorded and the time profile of heavy metal ions adsorption was plotted. After 90 min, the adsorbent removed the metal ions from the solution. Therefore, the optimum contact time for adsorption of the heavy metals was considered to be 90 min.

Equilibrium adsorption study

The equilibrium data were analyzed in accordance with the Langmuir, Frundlich, Redlich–Peterson, and Sips isotherm models.

The linear form of the Langmuir isotherm is [36]:

$$\frac{C_e}{q_e} = \frac{1}{K_L q_m} + \frac{1}{q_m} C_e \tag{4}$$

where K_L is a constant, C_e the equilibrium concentration (mg L^{-1}), q_e the amount of metal ions adsorbed per gram of adsorbent (mg g^{-1}) at equilibrium concentration C_e, and q_m is the maximum amount of solute adsorbed per gram of surface (mg g^{-1}), which depends on the number of adsorption sites. The Langmuir isotherm shows that the amount of solute adsorption increases as the concentration increases up to a saturation point.The linear form of Freundlich empirical model is represented by [37]:

$$\ln q_e = \ln k_f + \frac{1}{n} C_e \tag{5}$$

where K_f ($mg^{1-1/n} L^{1/n} g^{-1}$) and $1/n$ are Freundlich constants that depend on temperature and the given adsorbent–adsorbate couple. The parameter n is related to the adsorption energy distribution, and K_f indicates the adsorption capacity.The Redlich–Peterson [32] isotherm is an empirical isotherm incorporating three parameters. It combines elements from both the Langmuir and Freundlich equations, and the mechanism of adsorption is a hybrid and does not follow ideal monolayer adsorption:

$$q_e = \frac{K_R C_e}{1 + \alpha_R C_e^{\beta}} \tag{6}$$

where K_R is the Redlich–Peterson isotherm constant (L g^{-1}), α_R also a constant having unit of (mg^{-1}) and β is an exponent that lies between 0 and 1.

Sips isotherm [32] is a combined form of Langmuir and Freundlich expressions deduced for predicting the heterogeneous adsorption systems and circumventing the limitation of the rising adsorbate concentration associated with Freundlich isotherm model. At low adsorbate concentrations, it reduces to Freundlich isotherm, while at high concentrations, it predicts a monolayer adsorption capacity characteristic of the Langmuir isotherm:

$$q_e = \frac{q_m K_S C_e^{1/n}}{1 + K_S C_e^{1/n}} \tag{7}$$

where q_m is the Sips maximum adsorption capacity (mg g^{-1}), K_S the Sips equilibrium constant (L mg^{-1}), and $1/n$ is the Sips model exponent. After the equilibrium adsorption data were fitted with different isotherm models with nonlinear or linear regression, the fitting parameter values are as summarized in Table 1.

The higher correlation factors of Langmuir model ($R^2 > 0.99$) indicate that the Langmuir model gives a better fit to the experimental data and so the nature of adsorption of investigated cations on the ANMNPs is more compatible with Langmuir assumptions. Langmuir model does not take into account the variation in the adsorption energy, but it is the simplest description of the adsorption process. It is based on the physical hypothesis that the maximum

Table 1 Adsorption isotherm parameters for various two and three parameters adsorption isotherm models for the adsorption of investigated cations onto ANMNPS at 25 °C

Isotherm models	Parameters	Metal ions		
		Pb(II)	Cr(III)	Cd(II)
Langmuir	K_L (L g^{-1})	0.94	0.01	0.07
	q_m (mg g^{-1})	67.35	170.84	106.70
	R^2	0.994	0.999	0.998
Freundlich	K_f ($mg^{1-1/n}$ $L^{1/n}$ g^{-1})	36.33	2.80	19.99
	$1/n$	0.15	0.68	0.33
	R^2	0.949	0.983	0.876
Redilch–Peterson	K_R (L g^{-1})	8.09	1.05	7.08
	α_R	1.43	0.00	0.04
	β	0.954	2.15	1.06
	r^2	0.921	0.944	0.947
Sips	q_m (mg g^{-1})	73.31	87.85	86.43
	K_s	0.79	0.00	0.00
	$1/n$	0.68	3.43	3.05
	R^2	0.983	0.990	0.883

adsorption capacity consists of a monolayer adsorption, that there are no interactions between adsorbed molecules, and that the adsorption energy is distributed homogeneously over the entire coverage surface.

The adsorption capacities for the adsorption of Pb(II), Cd(II), and Cr(III) by the ANMNPs expressed by Langmuir coefficient q_m demonstrate that adsorption capacity increased in the sequence of Pb(II) < Cd(II) < Cr(III). The different adsorption capacities maybe due to disparity in cations radius and interaction enthalpy values [38].

Desorption experiments

Desorption of metal ions from adsorbent and regeneration of the adsorbent are an important issue in view of reusability of the adsorbent. For desorption studies, metal-adsorbed ANMNPs were first washed by ultrapure water to remove the unabsorbed metals loosely attached to the vial and adsorbent. In order to estimate the recovery of Cd(II), Cr(III), and Pb(II) from ANMNPs, desorption experiments with different reagents [0.1 mol L^{-1} HCl, 0.1 mol L^{-1} HNO_3 and mixture of methanol:0.1 mol L^{-1} HNO_3 (1:1 v/v)] were performed. After adsorption of metal ions, the adsorbent was magnetically separated. Then 4.0 mL of the effluents was added to the separated adsorbent. Samples were collected after 5, 10, 20, and 30 min contact times with the effluent to evaluate metal recovery by means of an atomic absorption spectrophotometer.

The results showed that the mixture of methanol with 0.1 mol L^{-1} HNO_3 is effective as a back-extractant and can be used for the quantitative recovery of the metal ions (Table 2).

In acidic solution, the N-atom donor which serves as an electron donor can be protonated, resulting in a positive charge that repels metal ions. Nevertheless, this can be beneficial to the back-extraction step, because lowering solution pH facilitates decomplexation of the metal ion from the sorbent. Desorption rate was found to be very rapid as almost 97 % desorption completed within 20–25 min for all metal ions.

Effect of the initial sample volume

Due to low concentrations of heavy metals, preconcentration was performed on large volumes of real samples. Hence, to explore the possibility of enriching low concentrations of analyte from large volumes by the procedure, the effect of sample volume on the recovery of Pb(II), Cr(III), and Cd(II) ions was also investigated. For this purpose, 20–600 mL of sample solutions containing 25.0 mg L^{-1} of Pb(II), Cr(III), or Cd(II) was used at optimum conditions (Fig. 5).

It was found that quantitative recovery (>97 %) was obtained for Pb(II), Cr(III), and Cd(II) up to a sample volume of 300 mL. In this experiment, 300 mL of sample solution was adopted for the preconcentration of Pb(II), Cr(III), or Cd(II) ions from water samples, the extracted Pb(II), Cr(III), or Cd(II) ions can be eluted with a mixture of 2 mL of 0.1 mol L^{-1} HNO_3 and 2 mL of methanol, so an enrichment factor of 75.0 is achieved by this method.

Table 2 Effect of different eluents on desorption recovery (%)

Eluent	Recovery (%)		
	Pb(II)	Cr(III)	Cd(II)
0.1 mol L^{-1} HCl	50.3	32.2	78.5
0.1 mol L^{-1} HNO_3	68.8	67.1	85.3
0.1 mol L^{-1} HNO_3 + methanol (1:1 v/v)	97.6	98.0	98. 3

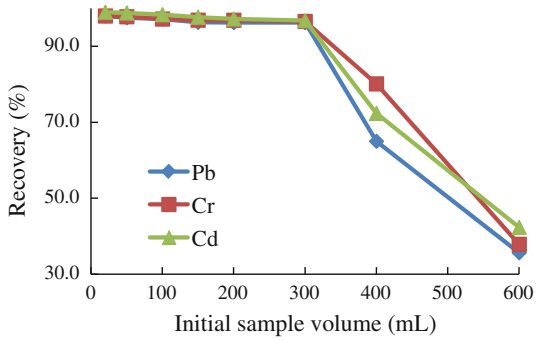

Fig. 5 Recovery percentage of investigated ions at different solution volumes. Conditions: pH 5, 0.03–0.07 g of adsorbent, 20–600 mL of sample solutions containing 25.0 mg L^{-1} of heavy metal ions, agitation time of 90 min and desorption using 4.0 mL from mixture of methanol:0.1 mol L^{-1} HNO_3 (1:1 v/v)

Table 3 Effects of the potentially interfering ions on the recoveries of the examined metal ions ($N = 3$)

Potentially interfering ions	Potentially interfering ion/analyte fold ratio	Recovery (%)		
		Pb(II)	Cd(II)	Cr(III)
Na^+	1,000	99.0 ± 0.1	98.0 ± 0.3	98.0 ± 0.1
Cl^-	1,000	100.3 ± 0.0	99.1 ± 0.1	99.4 ± 0.1
NO_3^-	3,500	97.1 ± 0.2	97.1 ± 0.2	98.1 ± 0. 5
Ca^{2+}	5,000	98.9 ± 0.1	97.6 ± 0.4	97.3 ± 0.0
SO_4^{2-}	3,000	99.5 ± 0. 5	99.9 ± 0.5	99.6 ± 0.1
Mg^{2+}	5,000	98.1 ± 0.4	99.3 ± 0.1	98.8 ± 0.4
Pb^{2+}	90	–	98.7 ± 0.2	99.7 ± 0.2
Cd^{2+}	80	97.0 ± 0.2	–	96.1 ± 0.1
Cr^{3+}	50	98.0 ± 0.1	97.7 ± 0.3	–
Fe^{2+}	60	99.3 ± 0.0	95.3 ± 0.1	97.5 ± 0.2
Co^{2+}	50	99.6 ± 0.2	98.5 ± 0.4	98.7 ± 0.5
Mn^{2+}	50	98.2 ± 0.5	98.0 ± 0.5	97.0 ± 0.2

Table 4 Analytical results for the determination of Pb(II), Cd(II), and Cr(III) in real samples

Sample	Meta ion	Added (ng mL^{-1})	Found (ng mL^{-1})	Recovery percent*
Tap water	Pb(II)	–	10.10	–
		10.00	20.23	101.3
	Cd(II)	–	0.30	–
		15.00	15.29	99.3
	Cr(III)	–	3.46	–
		20.00	23.35	99.5
Rice	Pb(II)	–	15.65	–
		10.00	25.81	101.6
	Cd(II)	–	2.93	–
		30.00	32.44	98.4
	Cr(III)	–	2.51	–
		40.00	41.89	98.5
KWC wastewater	Pb(II)	–	5.60	–
		40.00	46.10	101.2
	Cd(II)	–	1.36	–
		10.0	11.38	100.2
	Cr(III)	–	5.22	–
		20.0	25.24	100.1
Radiator manufacturing wastewater	Pb(II)	–	623.11	–
		50.00	673.30	100.4
	Cd(II)	–	8.34	–
		10.00	18.33	99.9
	Cr(III)	–	9.31	–
		30.00	39.10	99.3

* Values are based on triplicate analysis

Effect of potentially interfering ions

In view of the fact that FAAS provides high selectivity, the only interference may be attributed to the preconcentration step. The interfering effects of coexisting ions were studied on the percent recovery of target ions. The tolerance limit was set as the amount of potentially interfering ions required to cause a ±4 % error. To perform this study, various salts were added individually to a solution containing 25 mg L^{-1} of Pb(II), Cr(III), or Cd(II) ions, and the suggested procedure was applied. After adsorption of investigated ions, the adsorbed ions were eluted by eluent solution.

The content of target ions in effluents was determined using FAAS and the recoveries were calculated. Table 3 shows the tolerance limits of the interference ions. The results demonstrate that the presence of large amounts of species commonly present in real samples has no significant effect on the SPE of Pb(II), Cr(III), or Cd(II).

Analytical figures of merit

Under the optimum conditions, calibration curves were constructed for the determination of lead, cadmium and chromium according to the general procedure. Linearity was maintained between 1.30 and 900.00 ng mL^{-1} for lead(II), 0.50 and 300.00 ng mL^{-1} for chromium(III) and 0.30 and 150.00 ng mL^{-1} for cadmium(II), in 300 mL solution. The detection limit was determined as three times of the standard deviation (10 replicate measurements) of blank sample. The detection limits of this method, in the original solution, for Pb(II), Cd(II), and Cr(III) ions were 0.37, 0.03, and 0.21 ng mL^{-1}, respectively. As mentioned previously, the amount of target ions in 300 mL solution was measured after the elution of adsorbed ions by 4.0 mL of eluent; therefore, the maximum preconcentration factor for this method is 75.0.

Three replicate determinations of metal ions after preconcentration of 50 mL of 10.00 ng mL^{-1} Pb(II), Cd(II), and Cr(III) ions gave relative standard deviations of 0.94, 3.84, and 1.23 %, respectively. Calibration slopes increased proportionally, increasing the concentrated volume, which indicates that the retention/elution efficiency of the process is constant ($\sim$100 %).

Analysis of the real samples

The method has been applied to the determination of trace amounts of Pb(II), Cd(II), and Cr(III) ions in a wide variety

Table 5 Comparison of proposed method with some recent papers

Method[a]	Ions	Enrichment factor	Detection limit (ng mL^{-1})	Linear range (ng L^{-1})	Adsorption capacity (mg g^{-1})	References
Modified nanometer SiO_2 ICP-AES	Pb(II)	37.5	1.79	–	6.0	[39]
	Cr(III)		0.79	–	6.2	
SDS-PVC-BHABDI FAAS	Pb(II)	50.0	0.29	30–800	2.2	[40]
	Cr(III)		0.28	20–800	2.1	
	Cd(II)		0.37	10–700	2.8	
Diaion SP-850 resin FAAS	Pb(II)	50.0	0.5	–	–	[41]
	Cr(III)		0.65	–	–	
Solid sulfur FAAS	Pb(II)	250.0	3.2	10–300	0.0156	[42]
	Cd(II)		0.2	1–20	0.0034	
MMWCN FAAS	Pb(II)	120.0	0.32	0.83–15,000	9.3	[43]
	Cd(II)		0.04	0.17–3,000	1.0	
DNPH-nano-γ-Al_2O_3 FAAS	Pb(II)	266.7	0.43	1.2–350	100	[35]
	Cr(III)		0.55	2.4–520	100	
ANMNPs	Pb(II)	75.0	0.37	1.3–900	67.35	This work
	Cr(III)		0.21	0.5–300	170.84	
	Cd(II)		0.03	0.3–150	106.7	

[a] MMWCN modified multi-walled carbon nanotubes, SDS-PVC-BHABDI sodium dodecyl sulfate-coated poly(vinyl)chloride modified with bis(2-hydroxyacetophenone)-1,4-butanediimine, DNPH-nano-γ-Al_2O_3 2,4-dinitrophenylhydrazine-modified nano-Al_2O_3

of samples. The samples were also analyzed after spiking of analytes. Tap water, wastewater and rice samples were analyzed. The analytical results are presented in Table 4. In view of the high selectivity provided by FAAS, the recovery of spiked samples is satisfactory (in the range 98–101 %), which indicates the capability of the system in the determination of analytes in real samples with different matrices.

Conclusion

A simple, sensitive and selective method was developed for chemical modification of magnetite nanoparticles. And the ability of synthesized adsorbent for removal and preconcentration of Pb(II), Cd(II), and Cr(III) ions in various real samples was investigated. The synthesized nanoparticles were characterized using FT-IR, XRD, SEM, and TEM measurements.

The present method has the following advantages over the previously reported methods. Synthesized adsorbent is distinct in terms of sensitivity, selectivity toward the investigated metal ions. Also, these magnetic nanoparticles carrying the target metals could be easily separated from the aqueous solution simply by applying an external magnetic field; no filtration or centrifugation was necessary. Furthermore, the proposed method gives an efficient and cost-effective method with very low detection limits and good relative standard deviation and can be applied to determine the traces of these ions in various real samples. The maximum preconcentration factor, adsorption capacity and figures of merit achieved with the presented procedure are comparable with some SPE methods given in the literature (Table 5).

Acknowledgments The authors acknowledge the Bu-Ali Sina University Research Council and Center of Excellence in Development of Environmentally Friendly Methods for Chemical Synthesis (CEDEFMCS) for providing support to this work.

References

1. C. Huang, B. Hu, Spectrochim. Acta. B. **63**, 437 (2008)
2. V. Antochshuk, M. Jaroniec, Chem. Commun. 258 (2002)
3. M.R. Shishehbore, A. Afkhami, H. Bagheri, Chem. Cent. J. **5**, 41 (2011)
4. J. Huang, Y. Cao, Z. Liu, Z. Deng, F. Tang, W. Wang, Chem. Eng. J. **180**, 75 (2012)
5. A.F. Danil de Namor, A. El Gamouz, S. Frangie, V. Martinez, L. Valienta, O.A. Webb, J. Hazard. Mater. **241**, 14 (2012)
6. N. Burham, S.A. Azeem, M.F. El-Shahat, Cent. Eur. J. Chem. **7**, 945 (2009)
7. D. Atanassova, V. Stefanova, E. Russeva, Talanta. **47**, 1237 (1998)
8. O.M. EI-Hussaini, N.M. Rice, Hydrometallurgy. **72**, 259 (2004)
9. M. Soylak, M. Tüzen, D. Mendil, I. Turkekul, Talanta. **70**, 1129 (2006)
10. M. Soylak, L. Elci, J. Trace. Microprobe. Tech. **18**, 397 (2000)
11. M. Tuzen, I. Narin, M. Soylak, L. Elci, Anal. Lett. **37**, 473 (2004)
12. V. Strelko, D.J. Malik, M. Streat, Sep. Sci. Technol. **39**, 1885 (2004)
13. M. Kumar, D.P.S. Rathore, A.K. Singh, Microchim. Acta. **137**, 127 (2001)

14. J. Yin, Z.C. Jiang, G. Changm, B. Hu, Anal. Chim. Acta. **540**, 333 (2005)
15. J. Muńoz, J.R. Baena, M. Gallego, M. Valcárcel, J. Anal. At. Spectrom. **17**, 716 (2002)
16. A. Henglein, Chem. Rev. **89**, 1861 (1989)
17. R. Garro, M.T. Navarro, J. Primo, J. Catal. **233**, 342 (2005)
18. J.G. Hou, Q. Ma, X.Z. Du, H.L. Deng, J.Z. Gao, Talanta. **62**, 241 (2004)
19. P. Liang, B. Hu, Z.C. Jiang, Y.C. Qin, T.Y. Peng, J. Anal. At. Spectrom. **16**, 863 (2001)
20. T.K. Jain, I. Roy, T.K. De, A. Maitra, J. Am. Chem. Soc. **120**, 11092 (1998)
21. Y. Aoyama, T. Kanamori, T. Nakai, T. Sasaki, S. Horiuchi, S. Sando, T. Niidome, J. Am. Chem. Soc. **125**, 3455 (2003)
22. N. Murthy, Y.X. Thng, S. Schuck, M.C. Xu, J.M.J. Frechet, J. Am. Chem. Soc. **124**, 12398 (2002)
23. R.S. Faye, S. Aamdal, H.K. Hoifodt, Clin. Cancer Res. **10**, 4134 (2004)
24. J.C. Frias, Y.Q. Ma, K.J. Williams, Nano. Lett. **6**, 2220 (2006)
25. H.H. Yang, S.Q. Zhang, X.L. Chen, Z.X. Zhuang, J.G. Xu, X.R. Wang, Anal. Chem. **76**, 1316 (2004)
26. F. Wiekhorst, C. Seliger, R. Jurgons, J. Nanosci. Nanotechnol. **6**, 3222 (2006)
27. R. Hergt, R. Hiergeist, I. Hilger, J. Magn. Magn. Mater. **270**, 345 (2004)
28. J. Hu, G.H. Chen, M.C. Irene, Water Res. **39**, 4528 (2005)
29. X.L. Pu, Z.C. Jiang, B. Hu, H.B. Wang, J. Anal. At. Spectrom. **19**, 984 (2004)
30. A. Afkhami, M. Saber-Tehrani, H. Bagheri, T. Madrakian, Microchim. Acta. **172**, 125 (2011)
31. X.Q. Liu, Z.Y. Ma, J.M. Xing, H.Z. Liu, J. Magn. Magn. Mater. **270**, 1 (2004)
32. T. Madrakian, A. Afkhami, M. Ahmadi, Chemosphere. **90**, 242 (2013)
33. H. Keypour, M. Shayesteh, A. Sharifi-Rad, S. Salehzadeh, H. Khavasi, L. Valencia, J. Organomet. Chem. **693**, 3179 (2008)
34. B. Dai, M. Cao, G. Fang, B. Liu, X. Dong, M. Pan, S. Wang, J. Hazard. Mater. **219**, 103 (2012)
35. A. Afkhami, M. Saber-Tehrani, H. Bagheri, J. Hazard. Mater. **181**, 836 (2010)
36. T. Madrakian, A. Afkhami, M. Ahmadi, H. Bagheri, J. Hazard. Mater. **196**, 109 (2011)
37. T. Madrakian, A. Afkhami, H. Mahmood-Kashani, M. Ahmadi, J. Iran. Chem. Soc. **10**, 481 (2013)
38. M. Choi, J. Jang, J. Colloid. Interface. Sci. **325**, 287 (2008)
39. Y. Cui, X. Chang, Y. Zhai, X. Zhu, H. Zheng, N. Lian, Microchem. J. **83**, 35 (2006)
40. F. Marahel, M. Ghaedi, A. Shokrollahi, M. Montazerzohori, S. Davoodi, Chemosphere. **74**, 583 (2009)
41. M. Soylak, M. Tuzen, Diaion J. Hazard. Mater. **137**, 1496 (2006)
42. H. Parham, N. Pourreza, N. Rahbar, J. Hazard. Mater. **163**, 588 (2009)
43. S.Z. Mohammadi, D. Afzali, D. Pourtalebi, Cent. Eur. J. Chem. **8**, 662 (2010)